



HHS Public Access

Author manuscript

Med Image Comput Assist Interv. Author manuscript; available in PMC 2016 October 01.

Published in final edited form as:

Med Image Comput Assist Interv. 2015 October ; 9350: 169–176. doi:
10.1007/978-3-319-24571-3_21.

Identifying Connectome Module Patterns via New Balanced Multi-Graph Normalized Cut

Hongchang Gao¹, Chengtao Cai², Jingwen Yan², Lin Yan³, Joaquin Goni Cortes², Yang Wang², Feiping Nie¹, John West², Andrew Saykin², Li Shen², and Heng Huang^{1,★}

¹Computer Science and Engineering, University of Texas at Arlington, TX, USA

²Radiology and Imaging Sciences, Indiana University School of Medicine, IN, USA

³Department of Electronic Engineering, School of Electronic Information and Electrical Engineering, Shanghai Jiao Tong University, Shanghai, China

Abstract

Computational tools for the analysis of complex biological networks are lacking in human connectome research. Especially, how to discover the brain network patterns shared by a group of subjects is a challenging computational neuroscience problem. Although some single graph clustering methods can be extended to solve the multi-graph cases, the discovered network patterns are often imbalanced, *e.g.* isolated points. To address these problems, we propose a novel indicator constrained and balanced multi-graph normalized cut method to identify the connectome module patterns from the connectivity brain networks of the targeted subject group. We evaluated our method by analyzing the weighted fiber connectivity networks.

1 Introduction

To understand the mechanisms of human brain comprehensively, it is important to reveal the functioning of the brain network [9]. The emerging human connectome projects provide the fundamental insights into the organization and integration of brain networks, and greatly support the studies of brain circuitry and the understanding of human brain [9]. Each connectome is a comprehensive description of the network elements and connections that form the brain. In order to discover the full potential patterns of the connectome, the graph theory based models have been applied to reveal the architecture of the connectome [4, 11, 7]. In such a graph, nodes are neuroanatomical regions and edges are the density of the nerve fibers connecting the nodes. Analysis of the graph can disclose the topological structure, corresponding to a certain connectivity pattern in the connectome, which helps to understand the mechanisms of human brain.

To understand the underlying structural and functional mechanisms of the human brain, we need to discover the connectome module patterns which are shared by a group of subjects

Corresponding Author: heng@uta.edu.

★HG, FN, and HH were supported in part by IIS-1117965, IIS-1302675, IIS-1344152, DBI-1356628. CC, JY, AS, and LS were supported in part by NSF IIS-1117335, NIH UL1 RR025761, U01 AG024904, NIA RC2 AG036535, NIA R01 AG19771, NIH R01 LM011360, and NIA P30 AG1013318S1.

under the same conditions. However, the existing methods mostly focus on analyzing the connectome of individual subject rather than unifying them together [1, 8], which is not sufficient to find the shared network module patterns. The straightforward solution is to use the average connectivity networks of all subjects to detect the network module patterns. However, in such a method, some strong signals from individual networks could strongly influence the identified patterns. For example, if some networks have certain connections with high values, the average connectivity values of all networks will be dominated by these odd values and lead to the wrong patterns.

To address this challenging problem, we propose a new indicator constrained balanced multi-graph normalized cut method to identify the shared connectome module patterns from a group of subjects. The novelties of our proposed machine learning model are in three-fold: 1) The traditional normalized cut methods relax the discrete objectives to continuous formulation and require the k -means clustering as post-processing, which leads to sub-optimal results. We propose to utilize the clustering indicator matrix directly in our new objective such that the optimal results can be achieved; 2) Our new model can perform normalized cut on all connectivity networks simultaneously to identify the shared network patterns; 3) Because the connectivity networks are not fully connected graph, the naive multi-graph normalized cut model could find the biased patterns, such as the isolated nodes. To tackle this problem, we introduce a new regularization term for balanced normalized cut. We apply the proposed method to study the connectivity networks of four different subject groups: Health Control (HC), Significant Memory Concern (SMC), Mild Cognitive Impairment (MCI), and Alzheimer Disease (AD). In all empirical results, the top network module patterns identified by our method are more significant than the top modules detected by other related methods.

2 Methodology

The brain connectivity network can be represented as a graph $G = \{X, E, W\}$ with node set X , edge set E , and connectivity matrix W . Each node in X denotes an ROI (Region of Interest) in human brain. Each edge in E means that the end nodes (ROIs) of the edge are connective to each other. Each element in W denotes the density of the nerve fibers between a pair of nodes. Given m subjects under the same condition with n ROIs, we get m graph with m weight matrices W^1, W^2, \dots, W^m , where $W^k \in \mathfrak{R}^{n \times n}$, where W_{ij}^k is the density of nerve fibers between the i -th ROI and the j -th ROI in the k -th subject, where $k = 1, \dots, m, 1 \leq i, j \leq n$. Our goal is to discover the connectivity network patterns shared by the brain networks of all/most subjects. Traditional graph clustering methods can only deal with single graph, thus, we propose a novel balanced multi-graph normalized cut with indicator constraint algorithm to identify the shared network module patterns.

2.1 Balanced Multi-Graph Normalized Cut with Indicator Constraint

Given a connectivity matrix $W \in \mathfrak{R}^{n \times n}$, we can perform graph clustering on the network. Let $F = [f_1, f_2, \dots, f_c] \in \mathfrak{R}^{n \times c}$ as the cluster indicator matrix. The normalized cut model is to minimize $Tr(F^T L F)$ with the constraint $f_k = (0, \dots, 0, \frac{1}{\sqrt{f_k^T D f_k}}, \dots, \frac{1}{\sqrt{f_k^T D f_k}}, 0, \dots, 0)^T$ where $L = D - W$, and D is a diagonal matrix with $D_{ii} = \sum_j W_{ij}$. Minimizing this objective

function with such constraint is an NP hard problem [3]. The traditional method is to relax the desired discrete values to the continuous ones and solve the following problem:

$$\min_{F^T D F = I} Tr(F^T L F), \quad (1)$$

where elements of F are not discrete. Eq. (1) can be solved by the eigenvalue decomposition of the matrix L . After that, the discrete solution can be obtained by performing k -means clustering as post-processing, which converges to a local minimum and leads to suboptimal results. To address this problem, we propose a novel normalized cut method with indicator constraint to get the graph clustering results directly.

The normalized cut with indicator constraint is to minimize the following objective function:

$$\min_{F \in Ind} Tr(F^T L F), \quad (2)$$

where $F = [f_1, f_2, \dots, f_c] \in \mathbb{R}^{n \times c}$ is the group indicator matrix and c is the number of groups. The i -th element of f_k is set to 1 if the i -th node belongs to k -th group, otherwise 0. Because our solutions are clustering indicators, the final clustering results can be achieved directly without any post-processing step.

To discover the connectome module patterns on multiple graphs, we need perform the normalized cut on multiple graphs simultaneously. When the graph clustering model is performed on all networks, the corresponding nodes in each network should appear in the same group [6]. Thus, we force the group indicator matrices of all the networks to be the same matrix F . As a result, our multi-graph normalized cut objective is to solve:

$$\min_{F \in Ind} \sum_{v=1}^m Tr(F^T L^v F), \quad (3)$$

where $F \in \mathbb{R}^{n \times c}$ is the common group indicator matrix and m is the number of networks, L^v is the Laplacian matrix of the v -th connectivity network.

However, this model may identify isolated nodes as patterns, because many isolated nodes could be shared by all networks. Obviously, these isolated node patterns are not the correct ones. To avoid such a case, we introduce a new regularization term to guarantee a balanced multi-graph normalized cut as following:

$$\min_{F \in Ind} \sum_{v=1}^m Tr(F^T L^v F) + \gamma Tr(F^T 11^T F), \quad (4)$$

where $Tr(F^v 11^T F^v) = \sqrt{\sum_{j=1}^c (\sum_{i=1}^n \|f_{ij}^v\|)^2}$, which is the square-sum of the number of nodes in each group. To obtain the minimum of the square-sum of some numbers whose sum is fixed, these numbers should be equal to each other. Therefore, our proposed method combining both indicator constrained multi-graph normalize cut loss and balanced clustering regularization term, can achieve the balanced multi-graph clustering results.

2.2 Optimization Algorithm

In this paper, we solve the optimization problem via the Augmented Lagrangian Multiplier (ALM) method. We introduce an ancillary variable $G = F$ to obtain efficient updates on the optimization variables as following:

$$\min_{F \in \text{Ind}, G, F=G} \text{Tr}(F^T (\sum_{v=1}^m L^v + \gamma 11^T) G). \quad (5)$$

Next, we add a penalty term and a Lagrangian term to eliminate the constraints.

$$\min_{F \in \text{Ind}, G} \text{Tr}(F^T (\sum_{v=1}^m L^v + \gamma 11^T) G) + \text{Tr}(\Gamma^T (F - G)) + \frac{\mu}{2} \|F - G\|_F^2, \quad (6)$$

where $\Gamma \in \mathbb{R}^{n \times c}$ is the Lagrangian multiplier and μ is the regularity coefficient. It is equivalent to the following problem, because they have the same derivatives.

$$\min_{F \in \text{Ind}, G} \text{Tr}(F^T (\sum_{v=1}^m L^v + \gamma 11^T) G) + \frac{\mu}{2} \|F - G + \frac{1}{\mu} \Gamma\|_F^2. \quad (7)$$

The updating rules for F , G , Γ and μ are as following:

Update F—Optimizing Eq. (7) with respect to F is equivalent to optimizing

$$\min_{F \in \text{Ind}} \|F - C + \frac{1}{\mu} B\|_F^2. \quad (8)$$

where $B = AG$, $A = \sum_{v=1}^m L^v + \gamma 11^T$ and $C = G - \frac{1}{\mu} \Gamma$. Because each node belongs to only one group, there is only one element equal to one in each row. Thus, for i -th row, the solution of F_{ij} is:

$$F_{ij} = \begin{cases} 1 & \max_j (C_{ij} - \frac{1}{\mu} B_{ij}) \\ 0 & \text{otherwise} \end{cases} \quad (9)$$

Update G—Similar to optimize F , optimizing Eq. (7) with respect to G is equivalent to optimizing:

$$\min_G \text{Tr}(F^T AG) + \frac{\mu}{2} \|F - G + \frac{1}{\mu} \Gamma\|_F^2. \quad (10)$$

Taking the derivative w.r.t G and setting it equal to zero, we can get:

$$G = F - \frac{1}{\mu}(F^T A - \Gamma) \quad (11)$$

Update Γ and μ —At each iteration, we update μ and Γ as the following:

$$\Gamma = \Gamma + \mu(F - G), \mu = \rho\mu. \quad (12)$$

where ρ is a positive parameter to control the convergence speed. The above updating rules are repeated until convergence is achieved. Obviously, our proposed algorithm is convergent, because we divide the original optimization problem (7) into several subproblems and each of them is a convex optimization problem. Thus, by solving these subproblems alternatively, the proposed algorithm will guarantee the convergence.

3 Experiments and Discussions

3.1 Data Set and Network Construction

Data used in this work were obtained from the ADNI database (adni.loni.usc.edu). One goal of ADNI has been to test whether serial MRI, PET, other biological markers, and clinical and neuropsychological assessment can be combined to measure the progression of MCI and early AD. For up-to-date information, see www.adni-info.org. We downloaded baseline MRI and Diffusion Tensor Imaging (DTI) scans for 174 ADNI-GO/2 participants. Below we describe our method for constructing structural brain networks from MRI and DTI data.

1) ROI Generation—Anatomical parcellation was performed on the MRI scans using FreeSurfer 5.1 (<http://surfer.nmr.mgh.harvard.edu/>), coupled with Lausanne parcellation [5], to create 129 regions of interest (ROIs). Each MRI scan was registered to the low resolution b0 image of DTI data using the FLIRT tool-box in FSL (<http://www.fmrib.ox.ac.uk/fsl.html>), and the warping parameters were applied to the ROIs so that a new set of ROIs in the DTI image space were created. These new ROIs were used for constructing the structural network.

2) DTI Tractography—The DTI data were analyzed using FSL. Preprocessing included correction for motion and eddy current effects in DTI images. The processed images were then output to Diffusion Toolkit (<http://trackvis.org/>) for fiber tracking, using the streamline tractography algorithm called FACT (fiber assignment by continuous tracking). Quality control (QC) was performed via visual inspection, and 20 participants with questionable results were excluded.

3) Network Construction—The nodes were 129 ROIs obtained from parcellation. The edge weight is defined as the density of the fibers connecting the node pair, which is the number of tracks between two ROIs divided by the mean volume of two ROIs. A fiber is considered to connect two ROIs if and only if its end points fall in two ROIs respectively. The weighted network can be described by a matrix: The rows and columns correspond to the nodes, and matrix elements correspond to the edge weights.

3.2 Experiment Setup

Totally 154 participants (30 HC, 34 SMC, 62 MCI, and 28 AD) passed tractography QC and had networks constructed. We aimed to discover the connectome module patterns for each group. The scale of each network is 129×129 . We set the group number as 12. We used the normalized connectivity measure of connectome modules to evaluate the density of detected

modules: $D_{tt} = \frac{\sum_{v=1}^m s_{tt}^v}{m n_t}$, where D_{tt} is the normalized connectivity of the t -th module, m is the number of networks, n_t is the number of ROI in the t -th module M_t , $s_{tt}^v = \sum_{i \in M_t, j \in M_t} W_{ij}^v$ is the connectivity of the t -th module in the v -th network.

3.3 Comparison of Connectivity Measures

To evaluate the performance of our algorithm, we compared our algorithm with four other algorithms: (1) Spectral clustering on the average network (SC), performing the classical spectral clustering on the average of all the networks. (2) Multi-modal spectral clustering [2] (MMSC), which is to unify different networks from different subjects to perform spectral clustering. (3) Min-cut clustering (MCC), performing min-cut clustering on the average of all the networks. (4) Multi-graph minmax cut [10] (MGMC), performing minmax cut on each network and then unifying them together.

The connectivity measures of top 6 groups are shown in Table 1. Because the other four methods are not balanced clustering methods, some isolated nodes are identified as clusters (its corresponding normalized connectivity measure value is extremely high), which are not the significant patterns we expected. We view them as outliers and remove them. Thus, the result in Table 1 is the evaluation of the cluster with more than one node. Our results have no such cluster with isolated point, thus our method creates balanced results. As shown in Table 1, our method outperforms the other four methods in most cases. We performed T-test on the connectivity measures to evaluate the difference between our method and the others. As shown in Table 2, almost p value is less than 0.05, showing our method differently outperforms the other four methods.

3.4 Visualization of Detected Modules

To illustrate the grouping result, we visualized the top 6 connectome modules in Fig. 1. We mapped the modules to the mean networks, and visualized those from three different angles. Module 1 of HC, SMC and MCI groups were all located on the right hemisphere, including paracentral lobule, superior frontal gyri, and precuneus. Module 1 of AD group was, however, located on the left caudate and thalamus. For Module 2, both the HC and SMC groups had the clusters on the left hemisphere, where the HC group showed the pattern on hippocampus, amygdala, parahippocampal gyri, and temporal pole, and SMC on accumbens, frontal pole, medial orbital frontal, rostral anterior cingulate thickness, and superior frontal gyri thickness. The MCI group shared a similar pattern to SMC but on the right hemisphere. The AD group had the pattern on the right side including lingual gyri, pericalcarine gyri and superior parietal gyri. For Module 3, HC, SMC and MCI all had the clusters on the left hemisphere, including posterior cingulate, precuneus, and middle temporal gyri. The pattern

of AD group was located on the right frontal lobe, including superior frontal gyri, rostral middle frontal gyri and caudal middle frontal gyri.

4 Conclusion and Future Work

In this paper, we proposed a novel indicator constrained balanced multi-graph normalized cut method to detect the connectome module patterns shared by a group of subjects. We utilized a common indicator matrix to unify multiple graph clustering results directly, and introduced a new regularization term to make the graph clustering results balanced. Our method discovers the significant connectome modules for different brain disorder groups. These connectome modules can help other researchers on the variation studies of brain circuitries related to complex brain disorders. Our future work will also focus on identifying the genetic bases of these significant modules to enhance our understanding on the system biology of brain mechanism.

References

1. Bullmore E, Sporns O. Complex brain networks: graph theoretical analysis of structural and functional systems. *Nat Rev Neurosci.* 2009; 10(3):186–198. [PubMed: 19190637]
2. Cai, X.; Nie, F.; Huang, H.; Kamangar, F. Computer Vision and Pattern Recognition (CVPR), 2011 IEEE Conference on. IEEE; 2011. Heterogeneous image feature integration via multi-modal spectral clustering; p. 1977-1984.
3. Chan PK, Schlag MD, Zien JY. Spectral k-way ratio-cut partitioning and clustering. *Computer-Aided Design of Integrated Circuits and Systems, IEEE Transactions on.* 1994; 13(9):1088–1096.
4. Fornito A, Zalesky A, Breakspear M. Graph analysis of the human connectome: promise, progress, and pitfalls. *Neuroimage.* 2013; 80:426–44. [PubMed: 23643999]
5. Hagmann P, Cammoun L, Gigandet X, Meuli R, Honey CJ, Wedeen VJ, Sporns O. Mapping the structural core of human cerebral cortex. *PLoS Biol.* 2008; 6(7):e159. [PubMed: 18597554]
6. Kumar A, Rai P, Daume H. Co-regularized multi-view spectral clustering. *Advances in Neural Information Processing Systems.* 2011:1413–1421.
7. Nakagawa T, Jirsa V, Spiegler A, McIntosh A, Deco G. Bottom up modeling of the connectome: linking structure and function in the resting brain and their changes in aging. *Neuroimage.* 2013; 80:318–29. [PubMed: 23629050]
8. Rubinov M, Sporns O. Complex network measures of brain connectivity: uses and interpretations. *Neuroimage.* 2010; 52(3):1059–69. [PubMed: 19819337]
9. Sporns O, Tononi G, Kötter R. The human connectome: a structural description of the human brain. *PLoS computational biology.* 2005; 1(4):e42. [PubMed: 16201007]
10. Wang, D.; Wang, Y.; Nie, F.; Yan, J.; Cai, W.; Saykin, AJ.; Shen, L.; Huang, H. Medical Image Computing and Computer-Assisted Intervention–MICCAI 2014. Springer; 2014. Human connectome module pattern detection using a new multi-graph minmax cut model; p. 313-320.
11. Woolrich M, Stephan K. Biophysical network models and the human connectome. *Neuroimage.* 2013; 80:330–8. [PubMed: 23571421]

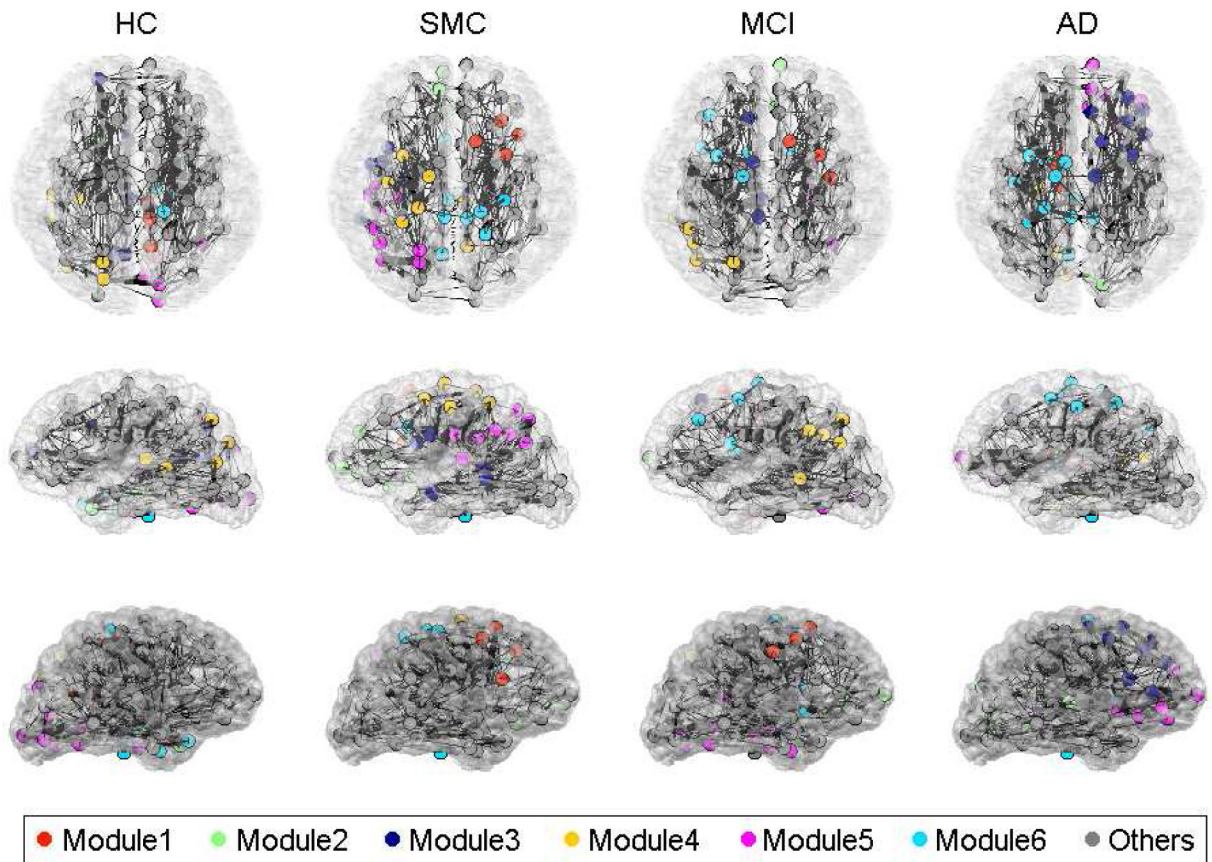


Fig. 1.

Top 6 connectome modules identified for each type. These modules are color-coded and mapped to the group mean networks. Line widths are proportional to the edge weights, where the maximum edge weight corresponds to the line width value of 1. Lines with their width values less than 0.1 are not plotted. Each row shows a visualization from a specific viewing angle.

Table 1

Connectivity measure on four types of subjects. SC denotes the results of spectral clustering on the average graph; MMSC denotes the results of multi-modal spectral clustering on all the graphs; MCC denotes the results of min-cut clustering on average graph; MGMC denotes the results of multi-graph minmax cut on all graphs.

#	(a) HC				(b) MCI						
	Our	SC	MMSC	MCC	MGMC	#	Our	SC	MMSC	MCC	MGMC
1	0.2557	0.1411	0.1926	0.1926	0.2496	1	0.2604	0.1907	0.1675	0.1186	0.2462
2	0.1926	0.1048	0.1639	0.1590	0.1781	2	0.2388	0.1578	0.1251	0.0998	0.1652
3	0.1777	0.0890	0.1531	0.1242	0.1401	3	0.2027	0.1550	0.1224	0.0948	0.1440
4	0.1573	0.0779	0.1422	0.0973	0.1399	4	0.1988	0.1309	0.1102	0.0909	0.1339
5	0.1428	0.0766	0.1205	0.0964	0.1330	5	0.1406	0.1003	0.1005	0.0894	0.1335
6	0.1339	0.0434	0.0964	0.0900	0.1315	6	0.0849	0.0899	0.0843	0.0825	0.1297
avg	0.1767	0.0888	0.1448	0.1266	0.1620	avg	0.1877	0.1375	0.1183	0.0960	0.1587

#	(c) AD				(d) SMC						
	Our	SC	MMSC	MCC	MGMC	#	Our	SC	MMSC	MCC	MGMC
1	0.2015	0.1860	0.1649	0.1312	0.1879	1	0.2791	0.1882	0.1671	0.1773	0.1640
2	0.1796	0.1296	0.1626	0.1024	0.1628	2	0.1790	0.0996	0.1668	0.1447	0.1494
3	0.1649	0.1071	0.1280	0.0980	0.1412	3	0.1783	0.0993	0.1503	0.1306	0.1436
4	0.1612	0.0921	0.1265	0.0950	0.1368	4	0.1582	0.0900	0.1399	0.1214	0.1425
5	0.1529	0.0799	0.1233	0.0943	0.1346	5	0.1487	0.0821	0.1301	0.1060	0.1393
6	0.1224	0.0659	0.1142	0.0811	0.1337	6	0.1306	0.0724	0.1266	0.0904	0.1292
avg	0.1638	0.1101	0.1365	0.1003	0.1495	avg	0.1790	0.1053	0.1468	0.1284	0.1447

Table 2

T-test between our method and other methods: p-values are shown.

Pair	HC	MCI	AD	SMC
Our-SC	0.00004	0.01060	0.00140	0.00002
Our-MMSC	0.00570	0.00940	0.00250	0.10500
Our-MCC	0.00010	0.00920	0.00006	0.00470
Our-MGMC	0.03510	0.17900	0.04550	0.09850

Author Manuscript

Author Manuscript

Author Manuscript

Author Manuscript